

Double photoionization of helium: Analysis of photoelectrons with respect to energies and angles

H. Le Rouzo

*Laboratoire de Photophysique Moléculaire du Centre National de la Recherche Scientifique,
Bâtiment No. 213, Université Paris-Sud, 91405 Orsay CEDEX, France
and Laboratoire de Physique Moléculaire, Faculté des Sciences, Boîte Postale No. 347, 51062 Reims CEDEX, France*

C. Dal Cappello

*Laboratoire de Physique Moléculaire et des Collisions, Faculté des Sciences,
Ile du Saulcy, 57045 Metz CEDEX 1, France*

(Received 31 May 1990)

The basic sixfold differential cross section $d^6\sigma^{2+}/d^3k d^3k'$ (SDCS) of the double photoionization process is derived within a "wave-function approach" (WFA) using a highly correlated ground-state wave function and a double-continuum final state approximated by a symmetrized product of one-electron Coulomb waves with \mathbf{k} and \mathbf{k}' asymptotic momenta. Relevant integrations of the SDCS are shown to provide a complete description of the $(\gamma, 2e)$ process. The theory is illustrated by calculations for helium targets: total cross sections, kinetic energy spectra, and angular plots of photoelectrons are presented. Considering the total cross section, it is found first that the agreement between the length and velocity result is worse than expected from the previous studies. In addition, the present model provides kinetic energy distributions of photoelectrons having the symmetry required by the Pauli principle. This is in contrast with earlier formulations of the WFA. For the SDCS, calculations have been done with final states where Coulomb waves were provided with either fixed charge ($Z=2$: unscreened nucleus) or variable effective charges. In the former case, it is found that the event where electrons escape with the same energy, along the polarization direction, has a significant probability. This deficiency is removed by use of angle-dependent effective charges since final-state correlation is partly accounted for in this way.

I. INTRODUCTION

The understanding of correlation effects arising in the dynamics of electrons escaping from a charged core is a permanent goal in atomic and molecular physics. Double photoionization (DPI) turns out to be a striking manifestation of this electron correlation since the simultaneous ejection of two electrons by a single photon would be forbidden if the independent-particle model were rigorously valid. Consequently, DPI is experimentally much less probable than single photoionization, usually by a factor of 100 for light species. Fortunately, the recent advent of intense and tunable synchrotron radiation has made possible the absolute measurement of total, i.e., *integrated*, cross sections $\sigma^{2+}(E_\gamma)$ as a function of the photon energy E_γ for atomic and molecular targets.¹ Very recently, and for the first time, two experiments have provided analyses in the angular and energy variables of the fragments ejected by DPI of atomic and molecular species: Huetz *et al.*² have measured the electrons ejected by the DPI of krypton close to threshold, while Kosmann *et al.*³ have investigated the angular distribution of H^+ ions resulting from the dissociative DPI of molecular hydrogen. At the same time, similar progress has been made in electron-atom collisions, the first $(e, 3e)$ experiments having just been performed by Lahmam-Bennani *et al.*⁴ with an argon target.

In face of this experimental interest in the double-ejection processes, the derivation of theoretical models that could predict the angular distribution of fragments in $(\gamma, 2e)$ and $(e, 3e)$ reactions becomes an urgent task. This goal is highly attractive since, by analogy with the (γ, e) and $(e, 2e)$ processes, one can expect that the *differential* cross sections will reveal dynamical information which is unavailable from the total cross sections alone. To this end, the present paper will deal with the description of the theoretical angular distribution of electrons ejected by photon impact, while a future paper⁵ will consider double ionization by fast electrons. For the sake of comparison, the formalisms derived in both papers will be illustrated by calculations for helium targets.

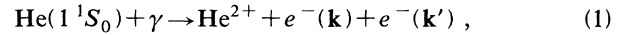
In fact, very few approaches are available currently for the theoretical description of multiple photoionization processes. In the vicinity of the threshold, the use of the Wannier-Rau-Peterkop (WRP) theory⁶ provides a very convenient approach. The hallmark of this theory is the predicted energy dependence of the cross section: e.g., it is found that the total DPI cross section of an atom varies above threshold as $\sigma^{2+} \propto E^m$, where E is the energy available for the two outgoing electrons, and m is an exponent depending on the charge Z of the residual ion. The theoretical values $m=1.127$ (for $Z=1$) and $m=1.056$ (for $Z=2$) are consistent with recent experiments done with H^- and K^- targets⁷ and He targets,⁸ re-

spectively. However, it should be noted that nearly equally satisfactory fits of experimental data can be made with the modulated linear law derived by Temkin⁹ with his Coulomb-dipole model. The WRP theory also provides valuable information on the angular distributions,¹⁰ but unfortunately, the validity of the threshold laws seems restricted to only a few eV above threshold.^{8,11} For the study of DPI over a larger energy range, say 200 eV above threshold, two main routes have been opened so far. The many-body perturbation theory (MBPT) has provided very accurate results¹² but only for atomic targets, probably due to the computational difficulties that would be highly increased by the noncentral molecular symmetry. On the other hand, the “wave-function approach” (WFA), first devised by Byron and Joachain¹³ (to be referred to as BJ) for the DPI of helium atoms, has been recently extended to the molecular hydrogen with encouraging results by Le Rouzo.^{14,15} The WFA rests essentially on a few basic assumptions (dipole approximation, nonrelativistic energies, neglect of non-Coulombic interactions, etc.) which are expected to be satisfied with a sufficient accuracy in the photon energy range mentioned above. Consequently, the validity of the WFA essentially depends on the quality of the wave functions used to describe both the initial (bound) and final (double continuum) states. Since highly accurate wave functions have long been obtained for the ground state of the helium atom, the major difficulty lies in the description of the double continuum states created by the DPI process. It is well known that the accurate description of the quantum motion of three charged particles is a permanent challenge for theoreticians. Analytical expressions of the corresponding wave function are available near threshold (WRP theory) and asymptotically, where all the interparticle distances are large.^{16,17} Since very little is known about the double-continuum wave functions over the entire space, the WFA usually makes use of final states represented within the independent-particle model,^{13–15,18} although a partly correlated double-continuum function has been used by Tiwary¹⁹ in order to evaluate the σ^{2+}/σ^+ ratio for the DPI of helium.

It should be stressed that, so far, both the MBPT and the WFA have only been applied to the calculation of DPI cross sections *integrated* over the angular variables, except for a preliminary work by Smirnov *et al.*,²⁰ who studied the electron correlations in $(\gamma, 2e)$ and $(e, 3e)$ reactions at high energies via the WFA provided with orthogonalized plane-waves. In this paper we investigate the *differential* cross sections for the $(\gamma, 2e)$ process. In order to extract the analysis of ejected electrons in the angular and energy variables, we have reexamined the WFA, and we propose a new formalism where the two ejected electrons, with \mathbf{k} and \mathbf{k}' as asymptotic momenta, are described by a symmetrized product of complex Coulomb waves for appropriate central charge Z . Note that this kind of wave function has been used by Tweed²¹ for the study of the double ionization of H^- , He , and Li^+ by electron impact.

In Sec. II, we present the general formalism of the new WFA. The basic equation of our approach is Eq. (22). This gives the essential sixfold differential cross section

$d^6\sigma^{2+}/d^3\mathbf{k}d^3\mathbf{k}'$ (SDCS) from which all other observables of the DPI process can be derived. As an illustration, we deduce the expression of the total cross section, and we show that some distributions of electron kinetic energy previously reported in the literature were not physically satisfactory. In Sec. III, computational details are given, especially concerning the description of the ground-state wave function for helium. In Sec. IV, our formalism is illustrated by calculations concerning the reaction



which, though relatively simple, is expected to display the main features of the basic DPI process, without the difficulties associated with structured cores. In order to take into account the dynamical screening of the nucleus by the escaping electrons, we also explore in this section the possible advantages that could result in using *effective* charges of the form $Z(\mathbf{k}, \mathbf{k}')$. Several choices of variable nuclear charge have been reported in the literature and have been employed for $(e, 3e)$ and $(e, 2e)$ studies.^{21,22}

II. GENERAL FORMALISM

A. The wave-function approach

We consider a DPI experiment where linearly polarized photons collide with helium atoms in their ground state. For a photon energy greater than the double-ionization threshold ($I^{2+} \simeq 79.0$ eV), the collision can result in the simultaneous ejection of two electrons having the asymptotic momenta \mathbf{k} and \mathbf{k}' in the laboratory frame. Our purpose is to evaluate the probability of this event, i.e., to derive the basic differential cross section $d^6\sigma^{2+}/d^3\mathbf{k}d^3\mathbf{k}'$. The expression of the differential cross section depends on the six variables used to express \mathbf{k} and \mathbf{k}' . In what follows, in order to allow easier comparisons with previous work, we shall use the energy $\varepsilon = k^2/2$ (in hartrees²³) as a variable, instead of the modulus k of the momentum $\mathbf{k} = (k, \hat{\mathbf{k}})$. With this convention, the sixfold differential cross section will read $d^6\sigma^{2+}/d\varepsilon d\varepsilon' d^2\hat{\mathbf{k}} d^2\hat{\mathbf{k}}'$, and will measure the basic probability of a double ionization where one electron is ejected with the energy ε (in the element $d\varepsilon$) along the direction $\hat{\mathbf{k}}$, (in the element of solid angle $d^2\hat{\mathbf{k}}$), while the other electron is ejected with ε' and $\hat{\mathbf{k}}'$, in the ranges $d\varepsilon'$ and $d^2\hat{\mathbf{k}}'$, respectively. Obviously, for an *atomic* target, the electronic energies $\varepsilon, \varepsilon'$ are not independent, so that one of them can be suppressed from the beginning. This convention, together with the use of the notation $d\hat{\mathbf{k}}$ for the two-variable solid-angle elements, has led to call triple differential cross section (TDCS) $d^3\sigma^{2+}/d\varepsilon d\hat{\mathbf{k}} d\hat{\mathbf{k}}'$ what we refer to as SDCS in the present work. We prefer to introduce the energy-conservation law via a Dirac distribution (see below) rather than suppressing one energy since this notation has been found more convenient for diatomic targets.²⁴

The SDCS is the *basic* observable of the collision since by convenient integrations, it provides a complete knowledge of the DPI process: (i) integrating twice over the energies ε and ε' yields the angular distribution of the pair of ejected electrons; (ii) integrating further over the

direction $\hat{\mathbf{k}}$ of one ejected electron allows the analysis of the angular distribution of the remaining electron along lines analogous to single photoionization (see, e.g., the role of the asymmetry parameter β); (iii) integrating only over the four angles \mathbf{k} and \mathbf{k}' provides the analysis of the photoelectrons in kinetic energy; and finally (iv) sixfold integration leads to the total cross section $\sigma^{2+}(E_\gamma)$.

Under the usual "electric dipole approximation," the differential cross section is proportional to the squared modulus of the dipole-matrix element $|M(\mathbf{k}, \mathbf{k}')|^2$ connecting the ground-state wave function ${}^1\Psi_i(1S_0|\mathbf{r}_1, \mathbf{r}_2)$ and the final-state wave function ${}^1\Psi_f(\mathbf{k}, \mathbf{k}'|\mathbf{r}_1, \mathbf{r}_2)$. The dipole-matrix elements are usually obtained, either in the length form (M_L) or in the velocity form (M_V), as integrals over all the positions \mathbf{r}_1 and \mathbf{r}_2 of the electrons.

For incident light linearly polarized along the z axis of the laboratory frame, these matrix elements are

$$M_L(\mathbf{k}, \mathbf{k}') = \langle {}^1\Psi_f(\mathbf{k}, \mathbf{k}') | z_1 + z_2 | {}^1\Psi_i(1S_0) \rangle, \quad (2a)$$

$$M_V(\mathbf{k}, \mathbf{k}') = \left\langle {}^1\Psi_f(\mathbf{k}, \mathbf{k}') \left| \frac{\partial}{\partial z_1} + \frac{\partial}{\partial z_2} \right| {}^1\Psi_i(1S_0) \right\rangle. \quad (2b)$$

The final-state wave functions and the dipole operators appearing in Eqs. (2) are conveniently expressed in the laboratory frame since the wave vectors of electrons and the polarization of the incident radiation refer to the space-fixed axis. After averaging over all the possible orientations of the target, it may be shown that the basic differential cross section for DPI by photons with energy E_γ is

$$\frac{d^6\sigma^{2+}(\mathbf{k}, \mathbf{k}' | E_\gamma)}{d\varepsilon d\varepsilon' d^2\hat{\mathbf{k}} d^2\hat{\mathbf{k}'}} = (4\pi^2\alpha a_0^2) E_\gamma |M_L(\mathbf{k}, \mathbf{k}')|^2 \delta(\varepsilon + \varepsilon' + I^{2+} - E_\gamma) \quad (3a)$$

$$= (4\pi^2\alpha a_0^2) \frac{1}{E_\gamma} |M_V(\mathbf{k}, \mathbf{k}')|^2 \delta(\varepsilon + \varepsilon' + I^{2+} - E_\gamma), \quad (3b)$$

where α is the fine-structure constant, a_0 is the Bohr radius, and the Dirac distributions ensure conservation of the total energy. As is well known, the results provided by Eqs. (3) would be identical if both wave functions entering in Eqs. (2) were exact. Alternatively, the discrepancy between the length and velocity cross sections gives a qualitative estimate of the accuracy of wave functions.

By definition, the WFA requires explicit knowledge of the initial- and final-state wave functions. An essential contribution of the work of BJ was to point out the necessity of including the electron correlation in the helium ground-state wave function. This point was soon confirmed by Brown,¹⁸ who used a better wave function for the helium ground state. Following these authors, we shall adopt here highly correlated wave functions whose description is deferred to Sec. III.

The singlet final-state wave functions will be described within the independent-particle model: if the electrons are placed in two different orbitals having definite momenta \mathbf{k} and \mathbf{k}' in the laboratory frame, the final-state wave functions read

$$\begin{aligned} & {}^1\Psi_f(\mathbf{k}, \mathbf{k}' | \mathbf{r}_1, \mathbf{r}_2) \\ &= \frac{1}{\sqrt{2}} [\psi(\mathbf{k} | \mathbf{r}_1) \psi(\mathbf{k}' | \mathbf{r}_2) + \psi(\mathbf{k}' | \mathbf{r}_1) \psi(\mathbf{k} | \mathbf{r}_2)]. \end{aligned} \quad (4)$$

It is well known that the spin part of two-electron wave functions can be factored out. Since, in addition, the very small spin-dependent interactions are neglected here, the spin can be ignored in the rest of this paper. Its sole manifestation is that the spatial parts of all wave functions are invariant under the exchange of the electron positions \mathbf{r}_1 and \mathbf{r}_2 , and that only singlet-singlet transitions

are allowed. The one-electron orbitals used to construct the final states are essentially pure Coulomb waves $\psi(\mathbf{k}, Z | \mathbf{r})$. These waves are the eigensolutions of the Schrödinger equation describing a continuum electron (i.e., with $\varepsilon \geq 0$) moving in the Coulomb field created by a charge Z . For photoionization, the relevant Coulomb waves are normalized using the incoming wave boundary condition.²⁵ With this normalization, the Coulomb wave has the asymptotic behavior of a plane wave (with a logarithmic distorted phase) plus an incoming spherical wave. It takes the form

$$\begin{aligned} \psi(\mathbf{k}, Z | \mathbf{r}) &= \frac{\sqrt{k}}{(2\pi)^{3/2}} e^{-\pi\eta/2} \Gamma(1 - i\eta) \\ &\times e^{i\mathbf{k}\cdot\mathbf{r}} F(i\eta, 1, -i(kr + \mathbf{k}\cdot\mathbf{r})), \end{aligned} \quad (5)$$

where $\eta = -Z/k$ and Γ and F are the well-known Γ and confluent hypergeometric functions, respectively.²⁶ For fixed central charge Z , Coulomb waves given in Eq. (5) are normalized according to

$$\langle \psi(\mathbf{k}, Z) | \psi(\mathbf{k}', Z) \rangle = \delta_{(\varepsilon - \varepsilon')} \delta_{(\hat{\mathbf{k}} - \hat{\mathbf{k}'})}. \quad (6)$$

Note that if $Z = 0$, the Coulomb waves reduce to the familiar plane waves $e^{i\mathbf{k}\cdot\mathbf{r}}$ within the relevant normalization factor $\sqrt{k} / (2\pi)^{3/2}$. Since pure plane waves suffer from major shortcomings, using orthogonalized plane waves has been suggested.²⁰ Both approximations are discussed in a future paper.⁵

As mentioned in the Introduction, the use of *variable* effective charges allows for screening of the residual ion. Let $Z(\mathbf{k}, \mathbf{k}')$ be the effective charge seen by an electron having momentum \mathbf{k} while the other electron has momentum \mathbf{k}' . The final-state wave function will then read

$${}^1\Psi_f(\mathbf{k}, \mathbf{k}' | \mathbf{r}_1, \mathbf{r}_2) = \frac{1}{\sqrt{2}} [\psi(\mathbf{k}, Z(\mathbf{k}, \mathbf{k}') | \mathbf{r}_1) \times \psi(\mathbf{k}', Z(\mathbf{k}', \mathbf{k}) | \mathbf{r}_2) + (\mathbf{r}_1 \leftrightarrow \mathbf{r}_2)] . \quad (7)$$

It is readily verified that interchange of electrons 1 and 2 still amounts to the interchange of the momenta \mathbf{k} and \mathbf{k}' . In other words, satisfying the Pauli principle implies the invariance of the final state upon the permutation of the momenta. For brevity, we shall use Z and Z' in place of $Z(\mathbf{k}, \mathbf{k}')$ and $Z(\mathbf{k}', \mathbf{k})$, respectively.

B. The partial-wave analysis

The evaluation of the partial cross sections presented in Sec. II A could be done by direct integration of the dipole-matrix elements. This method has been applied in a future paper⁵ dealing with the $(e, 3e)$ process. Alternatively, we here perform a partial-wave analysis of the wave functions. It will be shown that this technique provides a deeper insight into the $(\gamma, 2e)$ reaction, and will also allow us to make a closer contact with previous work involving the WFA. It has been pointed out²² that partial-wave analysis is not an efficient way to compute the $(e, 2e)$ differential cross sections. This is not true for DPI because the dipolar selection rules considerably reduce the useful part of the final-state wave function.

Coulomb waves [Eq. (5)] are not eigenvectors of the one-particle angular-momentum operators L^2 and L_z , i.e., they have no definite quantum numbers l and m . However,

er, they can be expanded in terms of partial waves $\phi(\varepsilon, l, m, Z | \mathbf{r})$ with well-defined quantum numbers l and m . These *spherical* Coulomb waves have the form

$$\phi(\varepsilon, l, m, Z | \mathbf{r}) = R_{\varepsilon l}^Z(r) Y_{lm}(\hat{\mathbf{r}}) , \quad (8)$$

with

$$R_{\varepsilon l}^Z(r) = \left[\frac{2}{k\pi} \right]^{1/2} \frac{F_l(\eta | kr)}{r} , \quad (9)$$

where $F_l(\eta | kr)$ is the regular spherical Coulomb function²⁶ of order l . Note that spherical Coulomb waves are normalized according to

$$\langle \phi(\varepsilon, l, m, Z) | \phi(\varepsilon', l', m', Z) \rangle = \delta_{(\varepsilon - \varepsilon')} \delta_{l, l'} \delta_{m, m'} \quad (10)$$

when the central charge Z is the same for both wave functions. The expansion of one-electron Coulomb waves [Eq. (5)] in terms of spherical waves is²⁵

$$\psi(\mathbf{k}, Z | \mathbf{r}) = \sum_{l=0}^{\infty} \sum_{m=-l}^{+l} i^l e^{-i\sigma_l(\eta)} Y_{lm}^*(\hat{\mathbf{k}}) \phi(\varepsilon, l, m, Z | \mathbf{r}) , \quad (11)$$

where the Coulomb phase shift is given by

$$\sigma_l(\eta) = \arg \Gamma(l + 1 + i\eta) . \quad (12)$$

Replacing the one-electron orbitals appearing in Eq. (7) by the partial-wave expansion given in Eq. (11) leads to

$${}^1\Psi_f(\mathbf{k}, \mathbf{k}' | \mathbf{r}_1, \mathbf{r}_2) = \sum_{l, m} \sum_{l', m'} i^{l+l'} e^{-i[\sigma_l(\eta) + \sigma_{l'}(\eta)]} Y_{lm}^*(\hat{\mathbf{k}}) Y_{l'm'}^*(\hat{\mathbf{k}}') \frac{1}{\sqrt{2}} [R_{\varepsilon l}^Z(r_1) R_{\varepsilon' l'}^{Z'}(r_2) Y_{lm}(\hat{\mathbf{r}}_1) Y_{l'm'}(\hat{\mathbf{r}}_2) + (1 \leftrightarrow 2)] , \quad (13)$$

where $(1 \leftrightarrow 2)$ means the preceding terms with 1 and 2 interchanged. In problems involving two directions it is customary to introduce the so-called *bipolar* harmonics,²⁷ i.e., the eigenstates of the total angular-momentum operators \mathbf{L}^2 and L_z

$$\mathcal{Y}_{LM}^{ll'}(\hat{\mathbf{r}}_1, \hat{\mathbf{r}}_2) = \sum_{m, m'} (l, m, l', m' | L, M) Y_{lm}(\hat{\mathbf{r}}_1) Y_{l'm'}(\hat{\mathbf{r}}_2) , \quad (14)$$

where $(l, m, l', m' | L, M)$ denotes the Clebsch-Gordan coefficients. Then, by use of standard manipulations of the algebra of angular momenta, Eq. (13) can be cast into the form

$${}^1\Psi_f(\mathbf{k}, \mathbf{k}' | \mathbf{r}_1, \mathbf{r}_2) = \sum_{L, M} \left[\sum_{l, l'} i^{l+l'} e^{-i[\sigma_l(\eta) + \sigma_{l'}(\eta)]} [\mathcal{Y}_{LM}^{ll'}(\hat{\mathbf{k}}, \hat{\mathbf{k}}')]^* \frac{1}{\sqrt{2}} [R_{\varepsilon, l}^Z(r_1) R_{\varepsilon', l'}^{Z'}(r_2) \mathcal{Y}_{LM}^{ll'}(\hat{\mathbf{r}}_1, \hat{\mathbf{r}}_2) + (1 \leftrightarrow 2)] \right] . \quad (15)$$

The form of the final-state wave function is now very convenient for proceeding further in the evaluation of the dipole-matrix elements: since the ground state is spherically symmetric, the dipole operators [Eqs. (2)] select the sole P_0 part ($L = 1, M = 0$) in the infinite expansions over L and M [Eq. (15)]. Moreover, the selection rules for the Clebsch-Gordan coefficients $(l, m, l', m' | 1, 0)$ suppress all the bipolar harmonics, except those of the form \mathcal{Y}_{10}^{l+1} and \mathcal{Y}_{10}^{l+1l} . As a consequence, the P_0 part of ${}^1\Psi_f(\mathbf{k}, \mathbf{k}')$ which is relevant for DPI is finally given by

$${}^1\Psi_f(P_0, \mathbf{k}, \mathbf{k}' | \mathbf{r}_1, \mathbf{r}_2) = \sum_{l=0}^{\infty} i^{2l+1} [e^{-i[\sigma_l(\eta) + \sigma_{l+1}(\eta)]} \mathcal{Y}_{10}^{l+1}(\hat{\mathbf{k}}, \hat{\mathbf{k}}')] {}^1\Phi_f(P_0, \varepsilon l Z, \varepsilon'(l+1) Z' | \mathbf{r}_1, \mathbf{r}_2) + (\mathbf{k} \leftrightarrow \mathbf{k}') , \quad (16)$$

where it is understood that the symbol $\mathbf{k} \leftrightarrow \mathbf{k}'$ means that energies, directions and consequently effective charges are to be interchanged. In Eq. (16), ${}^1\Phi_f(P_0, \varepsilon l Z, \varepsilon'(l+1) Z' | \mathbf{r}_1, \mathbf{r}_2)$ is the $M = 0$ component of the function

$${}^1\Phi_f(P_M, \varepsilon l Z, \varepsilon'(l+1)Z' | \mathbf{r}_1, \mathbf{r}_2) = \frac{1}{\sqrt{2}} \sum_{m=-l}^{+l} (l, m, l+1, M-m | 1, M) [\phi(\varepsilon, l, m, Z | \mathbf{r}_1) \phi(\varepsilon', l+1, M-m, Z' | \mathbf{r}_2) + (\mathbf{r}_1 \leftrightarrow \mathbf{r}_2)] . \quad (17)$$

It is important to mention that for $Z=Z'=\text{const}$, i.e., for a fixed nuclear charge, Eq. (17) exactly represents the double-continuum functions used previously for the calculations of the *integrated* cross sections of the DPI of He (Refs. 13 and 18) and H_2 .^{14,15} We shall establish a closer connection with these previous works in Sec. II C.

Inserting now the relevant part of the final-state wave function [Eq. (16)] into the dipole-matrix elements of Eqs. (2) leads to

$$M_{L,V}(\mathbf{k}, \mathbf{k}') = \sum_{l=0}^{\infty} (-i)^{2l+1} e^{i[\sigma_l(\eta) + \sigma_{l+1}(\eta')]} \mathcal{Y}_{10}^{l+1}(\hat{\mathbf{k}}, \hat{\mathbf{k}}') \mathcal{M}_{\varepsilon l Z, \varepsilon'(l+1)Z'}^{L,V} + (\mathbf{k} \leftrightarrow \mathbf{k}') , \quad (18)$$

where $\mathcal{M}^{L,V}$ denotes the matrix elements introduced by BJ

$$\mathcal{M}_{\varepsilon l Z, \varepsilon'(l+1)Z'}^L = \langle {}^1\Phi_f(P_0, \varepsilon l Z, \varepsilon'(l+1)Z' | z_1 + z_2 | {}^1\Psi_i(1S_0) \rangle , \quad (19a)$$

$$\mathcal{M}_{\varepsilon l Z, \varepsilon'(l+1)Z'}^V = \left\langle {}^1\Phi_f(P_0, \varepsilon l Z, \varepsilon'(l+1)Z' \left| \frac{\partial}{\partial z_1} + \frac{\partial}{\partial z_2} \right| {}^1\Psi_i(1S_0) \right\rangle . \quad (19b)$$

In view of future integrations, it is useful to have all arguments $\hat{\mathbf{k}}$ and $\hat{\mathbf{k}}'$ of the \mathcal{Y} 's in the same order. By use of the relation

$$\mathcal{Y}_{10}^{l+1}(\hat{\mathbf{k}}, \hat{\mathbf{k}}') = \mathcal{Y}_{10}^{l+1}(\hat{\mathbf{k}}', \hat{\mathbf{k}}) , \quad (20)$$

Eq. (18) is readily transformed into

$$M_{L,V}(\mathbf{k}, \mathbf{k}') = \sum_{l=0}^{\infty} (-i)^{2l+1} [e^{i[\sigma_l(\eta) + \sigma_{l+1}(\eta')]} \mathcal{Y}_{10}^{l+1}(\hat{\mathbf{k}}, \hat{\mathbf{k}}') \mathcal{M}_{\varepsilon l Z, \varepsilon'(l+1)Z'}^{L,V} + e^{i[\sigma_l(\eta') + \sigma_{l+1}(\eta)]} \mathcal{Y}_{10}^{l+1}(\hat{\mathbf{k}}, \hat{\mathbf{k}}') \mathcal{M}_{\varepsilon' l Z', \varepsilon(l+1)Z}^{L,V}] . \quad (21)$$

In order to express any n -fold differential cross section, one has finally to evaluate the squared modulus of the dipole-matrix elements [Eq. (21)]. Tedious but straightforward algebra leads to

$$\begin{aligned} |M_{L,V}(\mathbf{k}, \mathbf{k}')|^2 = & \sum_{l=0}^{\infty} \left\{ (\mathcal{M}_{\varepsilon l Z, \varepsilon'(l+1)Z'}^{L,V})^2 (\mathcal{Y}_{10}^{l+1})^2 + (\mathcal{M}_{\varepsilon(l+1)Z, \varepsilon' l Z'}^{L,V})^2 (\mathcal{Y}_{10}^{l+1})^2 \right. \\ & \left. + 2 \cos[\sigma_l(\eta) + \sigma_{l+1}(\eta') - \sigma_{l+1}(\eta) - \sigma_l(\eta')] \mathcal{M}_{\varepsilon l Z, \varepsilon'(l+1)Z}^{L,V} \mathcal{M}_{\varepsilon(l+1)Z, \varepsilon' l Z'}^{L,V} \mathcal{Y}_{10}^{l+1} \mathcal{Y}_{10}^{l+1} \right\} \\ & + 2 \sum_{l=0}^{\infty} \sum_{l'=l+1}^{\infty} (-1)^{l'-l} \left\{ \cos[\sigma_l(\eta) + \sigma_{l+1}(\eta') - \sigma_{l'}(\eta) - \sigma_{l'+1}(\eta')] \mathcal{M}_{\varepsilon l Z, \varepsilon'(l+1)Z}^{L,V} \mathcal{M}_{\varepsilon l' Z, \varepsilon'(l'+1)Z'}^{L,V} \mathcal{Y}_{10}^{l+1} \mathcal{Y}_{10}^{l'+1} \right. \\ & + \cos[\sigma_l(\eta) + \sigma_{l+1}(\eta') - \sigma_{l'+1}(\eta) - \sigma_{l'}(\eta')] \mathcal{M}_{\varepsilon l Z, \varepsilon'(l+1)Z}^{L,V} \mathcal{M}_{\varepsilon(l'+1)Z, \varepsilon' l' Z'}^{L,V} \mathcal{Y}_{10}^{l+1} \mathcal{Y}_{10}^{l'+1} \\ & + \cos[\sigma_{l+1}(\eta) + \sigma_l(\eta') - \sigma_{l'}(\eta) - \sigma_{l'+1}(\eta')] \mathcal{M}_{\varepsilon(l+1)Z, \varepsilon' l Z'}^{L,V} \mathcal{M}_{\varepsilon l' Z, \varepsilon'(l'+1)Z'}^{L,V} \mathcal{Y}_{10}^{l+1} \mathcal{Y}_{10}^{l'+1} \\ & + \cos[\sigma_{l+1}(\eta) + \sigma_l(\eta') - \sigma_{l'+1}(\eta) - \sigma_{l'}(\eta')] \\ & \left. \times \mathcal{M}_{\varepsilon(l+1)Z, \varepsilon' l Z'}^{L,V} \mathcal{M}_{\varepsilon(l'+1)Z, \varepsilon' l' Z'}^{L,V} \mathcal{Y}_{10}^{l+1} \mathcal{Y}_{10}^{l'+1} \right\} , \quad (22) \end{aligned}$$

where for the sake of compactness, the arguments of the \mathcal{Y} 's (always \mathbf{k} and \mathbf{k}' , in this order) have been suppressed. Introducing the expression of Eq. (22) into Eqs. (3) leads finally to the SDCS. Equation (22) is thus the basic result of the present formalism. It indicates how the angular distribution of electrons in double-ejection processes

is expressed in terms of matrix elements $\mathcal{M}^{L,V}$ previously evaluated in the WFA for the computation of integrated cross sections. The angular variables, i.e., the directions $\hat{\mathbf{k}}$ and $\hat{\mathbf{k}}'$, appear only in the bipolar harmonics which, in turn, are weighted by the matrix elements $\mathcal{M}^{L,V}$ depending on the electron energies. However, it should be em-

phasized that when direction-dependent effective charges are used, the angular variables are implicitly present in the matrix elements $\mathcal{M}^{L,V}$.

C. The integrated cross section

Since before this paper the WFA has essentially been applied to the calculation of integrated cross sections, it is instructive to make a comparison with previous work by deriving the expression for σ^{2+} . The total cross section is obviously obtained by the sixfold integration of the SDCS [Eqs. (3) together with Eq. (22)] over all energies

and directions. However, since the final-state wave function, and therefore the differential cross section, are invariant under the interchange of \mathbf{k} and \mathbf{k}' , straightforward angular integration over $(4\pi)^2$ steradians would count the same physical configuration twice. So, the correctly normalized total cross section is one half of the integral of the physically meaningful differential cross section²⁸

$$\sigma^{2+}(E_\gamma) = \frac{1}{2} \int d^6 \sigma^{2+}(\mathbf{k}, \mathbf{k}' | E_\gamma). \quad (23)$$

More explicitly, this yields

$$\sigma^{2+}(E_\gamma) = (4\pi^2 \alpha a_0^2) E_\gamma^{\pm 1} \frac{1}{2} \int d\varepsilon d\varepsilon' \delta(\varepsilon + \varepsilon' + I^{2+} - E_\gamma) \int d^2 \hat{\mathbf{k}} d^2 \hat{\mathbf{k}}' |M_{L,V}(\mathbf{k}, \mathbf{k}')|^2, \quad (24)$$

where E_γ or $1/E_\gamma$ corresponds to the length (M_L) or velocity (M_V) matrix elements, respectively. Now we can proceed to the fourfold integration over $d^2 \hat{\mathbf{k}}$ and $d^2 \hat{\mathbf{k}}'$. By use of the orthonormality of bipolar harmonics²⁷

$$\langle \mathcal{Y}_{LM}^{l_1 l_2} | \mathcal{Y}_{L'M'}^{l'_1 l'_2} \rangle = \delta_{l_1, l'_1} \delta_{l_2, l'_2} \delta_{L, L'} \delta_{M, M'}, \quad (25)$$

the integration of the complicated Eq. (22) is readily reduced to

$$\int d^2 \hat{\mathbf{k}} d^2 \hat{\mathbf{k}}' |M_{L,V}(\mathbf{k}, \mathbf{k}')|^2 = \sum_{l=0}^{\infty} [(\mathcal{M}_{\varepsilon l Z, \varepsilon'(l+1)Z}^{L,V})^2 + (\mathcal{M}_{\varepsilon(l+1)Z, \varepsilon' l Z}^{L,V})^2], \quad (26)$$

provided that the effective charges are fixed ($Z = Z' = \text{const}$). The considerable simplification, arising from the angular integration, is a striking illustration of the fact that the differential cross section is built up from a large number of very sensitive interference terms which vanish in the integrated cross section. The last step is now to integrate twice over the energy variables. For the DPI of an atomic target,²⁴ the energy conservation ensures that the total electronic energy E is a constant:

$$E = E_\gamma - I^{2+} = \varepsilon + \varepsilon'. \quad (27)$$

As a consequence the double integration over the energies reduces to a single integration over, say ε , while ε' is replaced by $E - \varepsilon$. This gives

$$\sigma^{2+}(E_\gamma) = (4\pi^2 \alpha a_0^2) E_\gamma^{\pm 1} \sum_{l=0}^{\infty} \int_0^E d\varepsilon \frac{1}{2} [(\mathcal{M}_{\varepsilon l Z, (E-\varepsilon)(l+1)Z}^{L,V})^2 + (\mathcal{M}_{\varepsilon(l+1)Z, (E-\varepsilon)lZ}^{L,V})^2]. \quad (28)$$

using the fact that, *after* integration, both terms between square brackets in Eq. (28) give the same contribution, this equation can be transcribed into

$$\sigma^{2+}(E_\gamma) = (4\pi^2 \alpha a_0^2) E_\gamma^{\pm 1} \sum_{l=0}^{\infty} \int_0^E d\varepsilon (\mathcal{M}_{\varepsilon l Z, (E-\varepsilon)(l+1)Z}^{L,V})^2. \quad (29)$$

Equation (29) is the expression derived by BJ and used in the previous applications of the WFA to DPI of helium^{13,18,19} and molecular hydrogen.^{14,15} To conclude, it is worth mentioning that this earlier version of the WFA provided the correct expression for the total cross section [Eq. (29)], but was unable to give differential spectra in energy and angular variables; furthermore, angular distributions were not available, since the angular variables had been discarded from the beginning in BJ's model. Moreover, it should be stressed that the integrand of Eq.

(29) does *not* provide a physically acceptable distribution of photoelectron kinetic energy $d\sigma^{2+}/d\varepsilon$, since this integrand is not symmetrical under the exchange of electron energies ε and $E - \varepsilon$, as required by the Pauli principle. In contrast, it is evident that in Eq. (28), the integrand exhibits the correct symmetry and so represents the proper kinetic-energy distribution. Of course, spectra in accordance with the symmetry requirement can always be extracted from the earlier unsymmetrical spectra, say $f(\varepsilon)$, by use of the transformation $\frac{1}{2}[f(\varepsilon) + f(E - \varepsilon)]$. However, since the correct energy spectra naturally occurs here, the formalism given in this paper is likely, in practice, to be more convenient than the previous one.

III. COMPUTATIONS

We turn now to the practical implementation of the theory presented in Sec. II. Computationally, the basic

moments calculated via Eq. (21) were introduced into the formulas giving the differential cross sections in both length and velocity forms [Eqs. (3)]. Phase shifts and bipolar harmonics are readily expressed²⁹ and coded, so that the main difficulty is the evaluation of the matrix elements \mathcal{M} given in Eqs. (19). In the case of molecular hydrogen, these matrix elements were evaluated numerically.¹⁵ Here, the central symmetry of the atomic problem allows the derivation of a closed analytical expression for the \mathcal{M} 's (Ref. 30) which has been thoroughly checked against the results provided by the previous numerical route described in Ref. 14. Our implementation follows the lines given in the work of BJ and of Tweed,²¹ but significant improvements have been achieved which are described below.

Firstly, consider the choice of the ground-state wave function. From symmetry considerations, it is easily shown that the wave function of any 1S_0 state of a two-electron atom can be written as

$$^1\Psi_i(S_0|\mathbf{r}_1, \mathbf{r}_2) = \sum_{l=0}^{\infty} \mathcal{Y}_{00}^l(\hat{\mathbf{r}}_1, \hat{\mathbf{r}}_2) \mathcal{R}_l(r_1, r_2), \quad (30)$$

where \mathcal{Y}_{00}^l is a bipolar harmonic defined in Eq. (14), and \mathcal{R}_l is a two-electron radial function symmetrical in the exchange of r_1 and r_2 . Wave functions of the self-consistent-field (SCF), configuration interaction (CI) and multiconfiguration self-consistent-field (MCSCF) types can be easily cast into the form of Eq. (30).

BJ obtained a ground-state wave function of helium with three "relative partial waves" corresponding to the ss , pp , and dd couplings of the electrons [$l=0, 1$, and 2 in Eq. (30)]. Their 45-parameter wave function gives an energy of -2.9020 hartrees, which indicates that 95.9% of the correlation energy³¹ is accounted for. In fact, since more compact and more highly correlated wave functions are available in the literature, we found it convenient to consider further functions of the CI and MCSCF types. In the preliminary stages of this work, several tests¹⁵ were made with the CI function proposed by Nesbet and Watson.³² However, the results presented here were obtained with a function fully optimized via the MCSCF method.³³ This function involves four "waves" up to the ff coupling ($l=0, 1, 2, 3$) and gives an energy of -2.90289 hartrees, so that 98.0% of the correlation energy is taken into account. In Sec. IV, the role played by the various components ss , pp , dd , and ff in the construction of the angular distribution of ejected electrons will be discussed. So it is worth mentioning that the ss , pp , dd , and ff "waves" account for 41, 51, 5, and 1% of the correlation energy, respectively. This shows that the radial correlation (41%) is less than the angular one, and that the angular correlation is mainly of the pp type. Inspection of these percentages along with the weights of each wave in the normalized ground-state function, i.e., 0.996 ($l=0$), 4.0×10^{-3} ($l=1$), 1.7×10^{-4} ($l=2$), and 1.7×10^{-5} ($l=3$), reveals that the dd wave contributes to the correlation energy (5%) much more significantly than what would be expected from its very feeble weight ($\leq 0.02\%$). In fact, it will be shown that this wave, left out by BJ in the calculation of transition moments, con-

tributes significantly to the cross sections, especially when the length form is used.

All the ground-state wave functions mentioned above are constructed with Slater-type one-electron orbitals. In this case, the radial parts of the ground-state wave functions read

$$\mathcal{R}_l(r_1, r_2) = \sum_{i,j} A_{i,j}^{(l)} [r_1^{m_i} r_2^{m_j} e^{-\alpha_i r_1} e^{-\alpha_j r_2} + (r_1 \leftrightarrow r_2)], \quad (31)$$

where the coefficients $A_{i,j}^{(l)}$ can be deduced from the wave functions reported in the literature. It should be noted that the form defined in Eq. (31) is more general than the previous ones^{13,21} in that the exponential terms of a given pair (i, j) here have different exponents. This improvement is known to give more highly correlated wave functions, but the price to be paid is a significant increase of the computational time required for the calculations of the matrix elements \mathcal{M} , especially when effective charges are employed.

Examination of the equations given in Sec. II reveals that the computation of the matrix elements \mathcal{M} amounts to the evaluation of basic radial integrals involving spherical Coulomb functions [Eq. (9)]

$$I_{\varepsilon l Z}^{\alpha \mu} = \int_0^{\infty} R_{\varepsilon l}^Z(r) e^{-\alpha r} r^{\mu} dr. \quad (32)$$

These integrals have been considered by several authors.³⁴ As a general rule, some integrals having special values of the integers l and μ are obtained in closed form, while the more complicated ones follow by recursion relations or by parametric differentiations with respect to the parameters ε or α . These procedures are somewhat cumbersome and are not computationally convenient for very accurate wave functions involving high quantum numbers. In order to avoid this problem, we have derived a closed analytical expression for the calculation of the $I_{\varepsilon l Z}^{\alpha \mu}$ integrals.³⁰ Finally, the analytical integration over the angles $\hat{\mathbf{r}}_1$ and $\hat{\mathbf{r}}_2$ leads, after some tedious but elementary Racah algebra, to the formulae for the matrix elements \mathcal{M} [Eqs. (19)] either in the length or in the velocity formulations. These expressions turn out to be finite linear combinations of products of two I integrals. The first few matrix elements have been given by BJ in the case where all exponents α are equal in the radial wave functions of Eq. (31).

The computational route described above has been coded and thoroughly checked: first, the total cross sections have been compared with the results of BJ and with our previous calculations¹⁵ obtained via a purely numerical route. On the other hand, the SDCS's derived via the present partial-wave approach have been compared with those resulting from the straightforward method developed in a future paper⁵ devoted to the double ionization of helium by electron impact. Since in the limit of vanishing momentum transfer, the generalized oscillator strength for the $(e, 3e)$ reaction reduces to the optical oscillator strength for the $(\gamma, 2e)$ process, we were able to proceed to the mutual control of our quite independent codes. Numerous tests have been made with moderately accurate CI ground-state wave functions of the ss ,³⁵ $ss+pp$,³⁵ and $ss+pp+dd$ (Ref. 36) types associated with

plane waves, with orthogonalized plane waves or with Coulomb waves for fixed and variable charges.

IV. RESULTS AND DISCUSSION

The formalism given in Sec. II was first applied to the calculation of the total cross section for the double photoionization of helium within the model used by BJ in their pioneering work.¹³ Using the 45-parameter ground-state wave function optimized by these authors and representing the ejected electrons by two Coulomb waves for the fixed central charge $Z=2$, we have performed the calculations of σ^{2+} , in both length and velocity formulation, as a function of the total electronic energy E . The results so obtained are represented by the thick curves in Fig. 1, where they can be compared with the cross sections of BJ (thin curves) recomputed by us. The striking discrepancy existing between the length form cross sections can be easily identified as the result of the truncation that BJ made in their ground-state wave function. In fact, for such a $ss+pp+dd$ initial state, the total cross section given in Eq. (29) can be rigorously expanded as

$$\sigma^{2+} = \sigma_{sp}^{2+}(ss;pp) + \sigma_{pd}^{2+}(pp;dd) + \sigma_{df}^{2+}(dd). \quad (33)$$

Equation (33) indicates that the contributions of the sp , pd , and df final-state partial waves [$l=0,1,2$ in Eq. (16)] are incoherently summed. On the other hand, due to the one-electron dipolar selection rules, each $l(l+1)$ partial

wave interacts both with the ll and the $(l+1)(l+1)$ parts of the initial state [Eq. (30)]. These two interactions are coherently added and give the contribution $\sigma_{l(l+1)}^{2+}(ll;(l+1)(l+1))$. However, note that the last term in Eq. (33) involves only a dd part since there is no f orbital in the considered initial function. The cross sections we have computed follow exactly the form given in Eq. (33), whereas BJ have discarded the dd contributions, probably because they could not do better with the limited computing facilities available at the time. This truncation of the ground-state wave function could at first sight appear reasonable, as the dd part of the ground state contributes for only 0.017% to the norm (see Sec. III). Hence, these authors have used the truncated expansion³⁷

$$\sigma^{2+} = \sigma_{sp}^{2+}(ss;pp) + \sigma_{pd}^{2+}(pp). \quad (34)$$

From Fig. 1, it can be seen that when all the terms of the ground-state function are included, the length curve is enhanced and its flattening disappears, while the velocity curve is slightly lowered. Unfortunately, in doing so, the ratio $\sigma_L^{2+}/\sigma_V^{2+}$, which should be 1 ideally, is worsened and takes now the value 2.6 instead of the value 1.8 for the incomplete calculation of BJ.

Having seen that even very small contributions to the ground-state wave function could play a significant role in DPI cross sections, we finally consider the highly accurate MCSCF function described in Sec. III. From the energetical point of view, 2.1% of correlation energy are gained with respect to the function used by BJ. The total cross sections for both these initial functions are shown in Fig. 2, together with the experimental data of Bizau

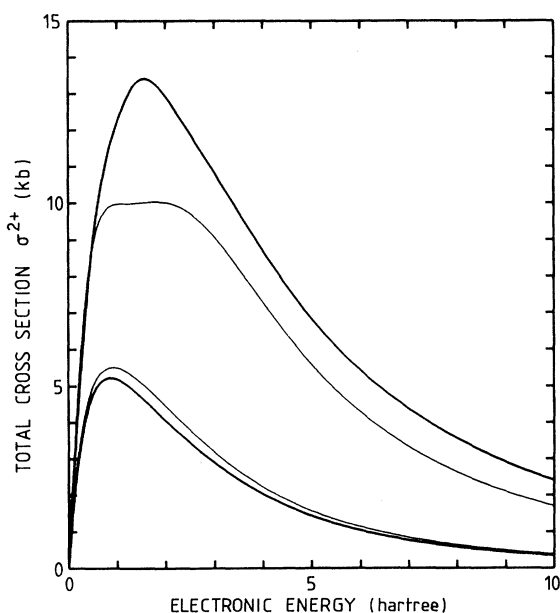


FIG. 1. The total cross section σ^{2+} for double photoionization of helium as a function of the total electronic energy ($1 \text{ kb} = 10^{-21} \text{ cm}^2$). The thin curves correspond to the calculations of Ref. 13, recomputed by us, whereas the thick curves represent the converged results within the same model (this work). Upper (lower) curves refer to the length (velocity) formulations.

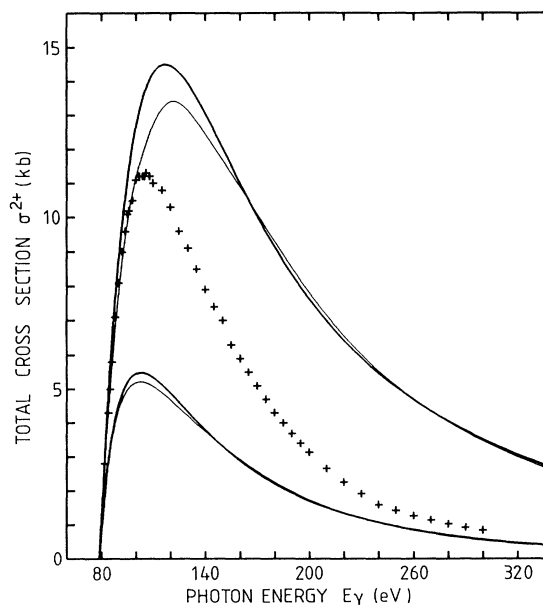


FIG. 2. The total cross section σ^{2+} for double photoionization of helium as a function of the photon energy ($1 \text{ kb} = 10^{-21} \text{ cm}^2$). The thick curves have been computed with the highly correlated MCSCF ground-state wave function, whereas the thin curves are for the ground state of BJ (the converged curves in Fig. 1). Experimental data points are from Bizau *et al.* (Ref. 38).

*et al.*³⁸ From this figure, one sees that the inclusion of correlation in the initial state enhances both the length and velocity cross sections in the region of the maximum. The ratio $\sigma_L^{2+}/\sigma_V^{2+}$ is scarcely modified (2.7 versus 2.6), but the positions of the L and V maxima become closer (120 and 106 eV, respectively). Considering now the experimental data, it can be seen that the length formulation is better close to the maximum, whereas the velocity formulation gives the correct behavior at high photon energy ($E_\gamma \geq 300$ eV), in accordance with the theoretical considerations of BJ.

In Fig. 3, some plots of electron kinetic-energy distributions $d\sigma^{2+}/d\varepsilon$ are made for photon energies 100, 109, 200, and 300 eV. These are the velocity results obtained with the MCSCF ground state and with $Z=2$ Coulomb waves. As explained in Sec. II, these plots have the proper symmetry, in accordance with the experimental results,³⁹ whereas the earlier version of the WFA leads to unsymmetrical kinetic-energy distributions. From Fig. 3 it is apparent that the mean value of $d\sigma^{2+}/d\varepsilon$ increases rapidly as the threshold region ($E_\gamma \geq 79$ eV) is approached in order that the integrated cross sections remain finite. At the same time, the kinetic-energy distribution tends to become flat. This trend is in accordance with the WRP theory which predicts that, near threshold, there is a constant probability that each electron carries off any fraction of the available energy. On the contrary, highly energetic photons favor the unequal sharing of the excess energy between the two photoelectrons. For

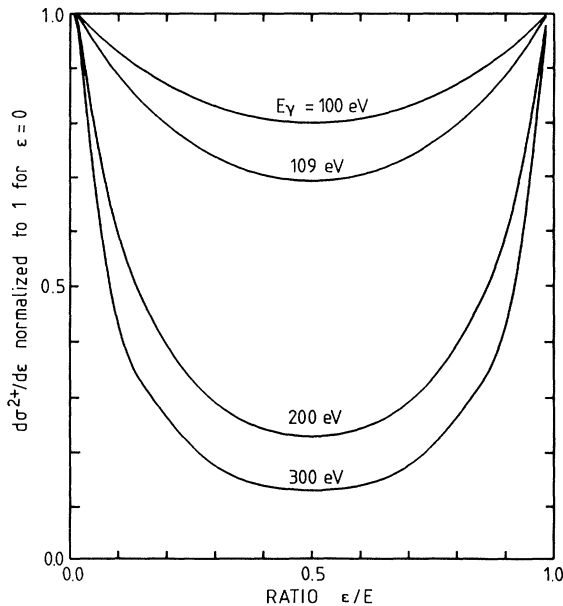


FIG. 3. The distribution of electron kinetic energy (velocity formulation) $d\sigma^{2+}/d\varepsilon$ as a function of the ratio ε/E : ε is the energy of an electron and E is the total available electronic energy. The distributions have been normalized to 1 for $\varepsilon=0$. For DPI of helium by 100-, 109-, 200-, and 300-eV impacting photons, E takes the values 21, 30, 121, and 221 eV, and the actual maxima (for $\varepsilon=0$) are 14.4, 0.73, 6.1, and 0.23 kb/hartree, respectively.

instance, with 300-eV photons, the probability of the event where one electron takes most of the available energy ($E \approx 220$ eV) while the other escapes slowly is about eight times greater than the probability for having both electrons ejected with the same energy $E/2 \approx 110$ eV.

We turn now to the SDCS calculated from Eqs. (3) and Eq. (22). We restrict ourselves to in-plane ionization for which \hat{e} , the polarization direction, and \mathbf{k}, \mathbf{k}' , the asymptotic momenta of photoelectrons, are coplanar. We consider two energy pairs $(\varepsilon, \varepsilon') = (15, 15)$ and $(5, 25)$ eV to be referred to as symmetric and asymmetric cases. Both correspond to the photon energy $E_\gamma = I^{2+} + 30$ eV ≈ 109 eV, which means that the pairs pertain to the region where the total cross section, in either the length or the velocity formulations, is large (see Fig. 2). Taking \mathbf{e} as the polar axis, and given a fixed direction for \mathbf{k} , the SDCS can be plotted as a function of the direction \mathbf{k}' . Such polar plots are displayed in Figs. 4 and 5 for the symmetric and asymmetric cases, respectively. From left to right, the three fixed directions \mathbf{k} are at 0, 45, and 90 deg with respect to the field direction. The upper and lower graphs refer to the length and velocity formulation, respectively. These plots have been obtained with pure Coulomb waves for $Z=2$ central charge and with the MCSCF ground-state wave function. In order to determine the relative influence of radial and angular correlation, we have plotted in Figs. 4 and 5 the SDCS obtained with the exact MCSCF ground state (thick curve) and those corresponding to the sole ss part of the MCSCF wave function (thin curve). As expected, it can be seen that without angular correlation, i.e., with only the ss part of the initial wave function, electrons are likely to be ejected along the polarization direction. Moreover, the shapes of the SDCS computed via the velocity formulation are rather insensitive to the introduction of ground-state angular correlation. This could make the velocity formulation somewhat questionable. On the contrary, in the length formulation, accounting for the $pp + dd + ff$ couplings in the initial wave function dramatically modifies the directions and intensities of the SDCS's lobes. In this case, electrons are no longer ejected near to the field direction, but escape in rather different directions. For instance, when one electron is detected at right angles to the polarization, one finds that the second one is likely to be observed along two symmetrical directions at 130 deg from the first electron. Curiously, this is a configuration very similar to that predicted by the WRP theory, at low energy. When the first electron is detected at 45 deg from the electric field, the fixed-charge model predicts that the second electron is ejected near the \hat{e} or \hat{k} directions, depending on the formulation of the dipole approximation. Finally, the event where one electron is detected along the direction field is found to be the most probable among all the coplanar configurations. In this case, all calculations predict that the second electron tends to escape in the same direction. For the symmetric case ($\varepsilon = \varepsilon' = 15$ eV) this means that electrons would be in the same spatial position simultaneously. Since the electrons have opposite spins (the final state is a singlet), the exclusion principle does not prevent this configuration. However, it should be remembered that the electronic

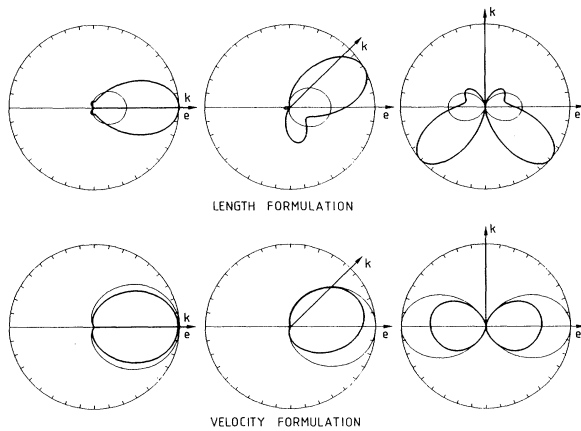


FIG. 4. The sixfold differential cross section (SDCS) $d^6\sigma^{2+}/d\epsilon d\epsilon' d^2\hat{\mathbf{k}} d^2\hat{\mathbf{k}}'$ for DPI of helium in coplanar geometries. Electron energies are $\epsilon = \epsilon' = 15$ eV. SDCS's are plotted as functions of the direction $\hat{\mathbf{k}}'$ of one electron, for three fixed directions $\hat{\mathbf{k}}$ (0° , 45° , and 90°) of the other one (the polar axis is the direction $\hat{\mathbf{e}}$). Coulomb waves have the fixed charge $Z=2$. Thick curves refer to the MCSCF ground-state wave function ($ss + pp + dd + ff$), thin curves are for the sole ss part. Upper (lower) plots correspond to the length (velocity) dipole formulation. The radius of each circle is the maximum of the calculated SDCS. In kb/hartree^2 units, these radii are 0.82, 0.47, and 0.18 (L formulation), and 0.21, 0.15, and 0.05 (V formulation).

repulsion $1/r_{12}$ between the ejected electrons is neglected in our model. Taking this correlation into account would necessarily modify this prediction.

To this end, and as a final consideration, it is of interest to examine the effect of variable charges $Z(\mathbf{k}, \mathbf{k}')$ on the angular distributions of photoelectron pairs. We have given the Coulomb waves the effective charges described in a future paper,⁵ and we have further orthogonalized these one-electron waves to the $1s$ ($Z=2$) hydrogenic or-

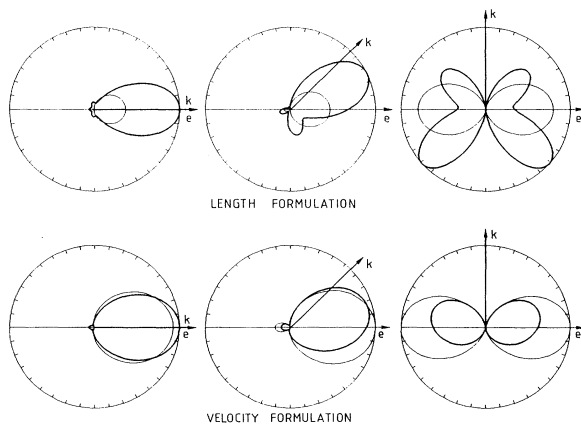


FIG. 5. As for Fig. 4, but with electron energies $\epsilon = 5$ eV and $\epsilon' = 25$ eV. In atomic units, the radii of circles are 0.90, 0.55, and 0.16 (upper, L formulation), and 0.24, 0.18, and 0.09 (lower, V formulation).

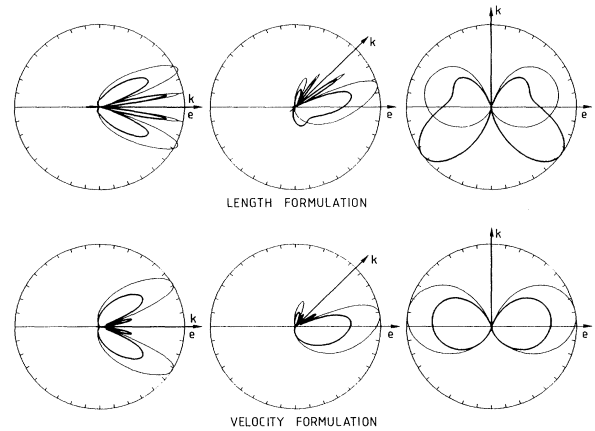


FIG. 6. As for Fig. 4, but Coulomb waves have the angular-dependent effective charge of Refs. 21 and 22 ($\epsilon = \epsilon' = 15$ eV). In atomic units, the radii of circles are 2.0, 1.6, and 0.30 (upper, L formulation), and 0.57, 0.48, and 0.11 (lower, V formulation).

bit. Since the $1s$ function is of short range, this procedure preserves the asymptotic behavior of the Coulomb wave but makes it more adequate since, in an independent-particle model, all one-electron orbitals are orthogonal [note that this procedure was introduced by Tweed²¹ in the $(e, 3e)$ context]. In Figs. 6 and 7, the SDCS's calculated with variable charges are displayed for the same dynamical parameters as in Figs. 4 and 5. The striking effect arising from the use of effective charges is the interdiction of the double ejection of electrons having the same momenta. This follows directly from the fact that $Z(\mathbf{k}, \mathbf{k}') \rightarrow -\infty$, and so $d\sigma^{2+} \rightarrow 0$ when $\mathbf{k} \rightarrow \mathbf{k}'$. As a consequence, the main lobes which had the intensities 0.82 and 0.21, for the L and V forms, respectively (see Fig. 4), split into two symmetric lobes about the directions ± 30 deg and having the intensities 1.30 (L) and

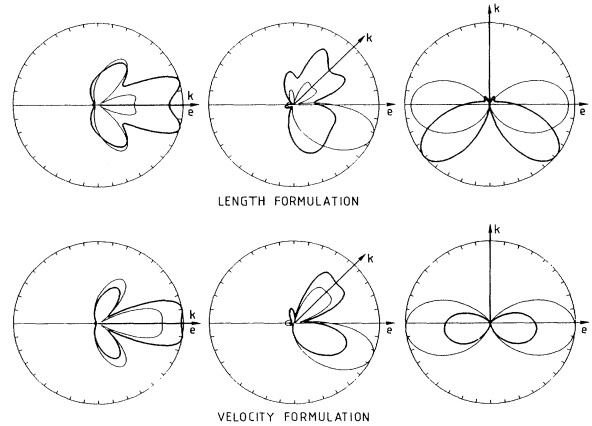


FIG. 7. As for Fig. 6, but with electron energies $\epsilon = 5$ eV and $\epsilon' = 25$ eV. In atomic units, the radii of circles are 0.88, 0.62, and 0.25 (upper, L formulation), and 0.40, 0.27, and 0.11 (lower, V formulation).

0.35 (V). Simultaneously, the SDCS's exhibit a pair of intense and narrow lobes that could be artifacts arising from the orthogonalization process. Hence, for the configuration $\mathbf{k}=\mathbf{k}'\propto e$, which probably represents the most stringent test of the model, the L/V ratio is scarcely improved by use of variable charges in place of $Z=2$ (3.7 versus 3.9). The situation is better for the asymmetric case and for other configurations, so that it remains possible that effective charges could be useful, on average, for the WFA.

V. CONCLUSIONS

In this paper, a fresh look has been taken at the WFA, which has been generalized in order to provide a *complete* description of the $(\gamma, 2e)$ process [a similar problem for the $(e, 3e)$ reaction will be considered in a future paper⁵]. Total cross section, photoelectron kinetic-energy distribution, and the basic SDCS (two energies, four angles) are derived within a formalism where the continuum electrons are described by a product of two Coulomb waves. In fact, this representation of the final states could be the major limitation of the present work, since the other model assumptions are quite reliable, and the ground state of helium is described by a highly accurate wave function taking into account more than 98% of the correlation energy.

The first manifestation of the lack of correlation in the final states is that the ratio $\sigma_L^{2+}/\sigma_V^{2+}$, which should be 1 ideally, is worse than expected from the pioneering work of BJ, whose calculations were not complete. Another questionable prediction of the model is that, for fixed effective charges Z , the most probable event in the DPI of helium by a linearly polarized light would be the ejection of both electrons in the direction of the electric field. Although this result corresponds to an energy of 30 eV above threshold, it is surprising to obtain a prediction in disagreement with the result given by the WRP theory.

In fact, this is the consequence of the complete neglect of electronic correlation in the double-continuum state. By use of *angle dependent* effective charges, the mutual screening of the nucleus by the ejected electrons is introduced. In this way, the final-state electronic correlation is partly accounted for and electrons actually depart in different directions.

Still within the WFA, we plan to improve the description of the DPI process by introducing correlation either implicitly, e.g., by use of better effective charges, or explicitly, e.g., via the variational R -matrix theory.⁴⁰ An alternative route, first suggested by Redmond,¹⁷ is to improve the double-continuum wave function via a multiplicative factor representing the relative motion of the electrons, i.e., a Coulomb wave for the interelectronic distance r_{12} . This three-body Coulomb wave function can be used either directly, as done very recently by Brauner *et al.*,⁴¹ or in its partial-wave expansion proposed by Altick,¹⁶ since Peterkop⁴² has proved that Redmond's and Altick's forms are equivalent.

Note added in proof. The fact that the energy distribution of the two outgoing electrons is flat, within 20%, at 20 eV above threshold (see Fig. 3) has just been experimentally confirmed by new coincidence measurements made by Lablanquie *et al.* [P. Lablanquie, K. Ito, P. Morin, I. Nenner, and J. H. D. Eland, *Z. Phys. D* **16**, 77 (1990)].

ACKNOWLEDGMENTS

We express our gratitude to Professor C. Tavard for suggesting this problem. We are grateful to Dr. J.-P. Gauyacq, Professor R. Lefebvre, and Dr. M. Raouf for helpful discussions and to Dr. H. Lefebvre-Brion, Dr. G. Raseev, and Dr. R. J. Tweed for the critical reading of the manuscript.

¹See the papers quoted in Ref. 15 and the following additional references: V. Schmidt, N. Sandner, H. Kuntzemüller, P. Dhez, F. Wuilleumier, and E. Källne, *Phys. Rev. A* **13**, 1748 (1976); D. M. P. Holland, K. Codling, J. B. West, and G. V. Marr, *J. Phys. B* **12**, 2465 (1979); T. Masuoka and J. A. R. Samson, *J. Chim. Phys.* **77**, 623 (1980); G. Dujardin, M.-J. Besnard, L. Hellner, and Y. Malinovitch, *Phys. Rev. A* **35**, 5012 (1987); P. Lablanquie, J. H. D. Eland, I. Nenner, P. Morin, J. Delwiche, and M. J. Hubin-Franskin, *Phys. Rev. Lett.* **58**, 992 (1987); S. D. Price and J. H. D. Eland, *J. Phys. B* **22**, L153 (1989); *ibid.* **23**, 2269 (1990).

²A. Huetz, P. Selles, and J. Mazeau (unpublished).

³H. Kossmann, O. Schwarzkopf, B. Kämmerling, and V. Schmidt, *Phys. Rev. Lett.* **63**, 2040 (1989).

⁴A. Lahmam-Bannani, C. Dupré, and A. Duguet, *Phys. Rev. Lett.* **63**, 1582 (1989).

⁵C. Dal Cappello and H. Le Rouzo (unpublished).

⁶G. H. Wannier, *Phys. Rev.* **90**, 817 (1953); A. R. P. Rau, *Phys. Rev. A* **4**, 207 (1971); R. Peterkop, *J. Phys. B* **4**, 513 (1971). A comprehensive review of the Wannier-Rau-Peterkop theory, by F. H. Read, can be found in *Electron Impact Ionisation*,

edited by T. D. Märk and G. H. Dunn (Springer, Berlin, 1985).

⁷J. B. Donahue, P. A. M. Gram, M. V. Hynes, R. W. Hamm, C. A. Frost, H. C. Bryant, K. B. Butterfield, D. A. Clark, and W. W. Smith, *Phys. Rev. Lett.* **48**, 1538 (1982); Y. K. Bae and J. R. Peterson, *Phys. Rev. A* **37**, 3254 (1988).

⁸H. Kossmann, V. Schmidt, and T. Andersen, *Phys. Rev. Lett.* **60**, 1266 (1988); G. C. King, M. Zubek, P. M. Rutter, F. H. Read, A. A. MacDowell, J. B. West, and D. M. P. Holland, *J. Phys. B* **21**, L403 (1988).

⁹A. Temkin, *Phys. Rev. A* **30**, 2737 (1984).

¹⁰P. L. Altick, *J. Phys. B* **18**, 1841 (1985); D. S. F. Crothers, *ibid.* **19**, 463 (1986); P. Selles, J. Mazeau, and A. Huetz, *ibid.* **20**, 5183 (1987); P. L. Altick and T. Rösel, *ibid.* **21**, 2635 (1988).

¹¹T. A. Roth, *Phys. Rev. A* **5**, 476 (1972).

¹²T. N. Chang, T. Ishihara, and R. T. Poe, *Phys. Rev. Lett.* **27**, 838 (1971); T. N. Chang and R. T. Poe, *Phys. Rev. A* **12**, 1432 (1975); S. L. Carter and H. P. Kelly, *ibid.* **16**, 1525 (1977); **24**, 170 (1981).

¹³F. W. Byron and C. J. Joachain, *Phys. Rev.* **164**, 1 (1967).

¹⁴H. Le Rouzo, *J. Phys. B* **19**, L677 (1986).

- ¹⁵H. Le Rouzo, Phys. Rev. A **37**, 1512 (1988).
- ¹⁶P. L. Altick, Phys. Rev. A **21**, 1381 (1980); **25**, 128 (1982); J. Phys. B **16**, 3543 (1983).
- ¹⁷P. J. Redmond (unpublished), quoted by L. Rosenberg, Phys. Rev. D **8**, 1833 (1973). See also the derivation of Ref. 41.
- ¹⁸R. L. Brown, Phys. Rev. A **1**, 586 (1970).
- ¹⁹S. N. Tiwary, J. Phys. B **15**, L323 (1982).
- ²⁰Y. F. Smirnov, A. V. Pavlitchenkov, V. G. Levin, and V. G. Neudatchin, J. Phys. B **11**, 3587 (1978). See also V. G. Levin, V. G. Neudatchin, A. V. Pavlitchenkov, and Y. U. Smirnov, *ibid.* **17**, 1525 (1984).
- ²¹R. J. Tweed, J. Phys. B **6**, 270 (1973).
- ²²M. Schulz, J. Phys. B **6**, 2580 (1973).
- ²³In atomic units $m = \hbar = |e| = 1$. Atomic units for length and energy are 1 bohr = 0.529 177 Å and 1 hartree = 27.211 65 eV, respectively. See B. N. Taylor, W. H. Parker, and D. N. Langenberg, Rev. Mod. Phys. **41**, 477 (1969).
- ²⁴For a molecular target like H₂, the conserved total energy reads $E = E_n + \epsilon + \epsilon'$, where E_n is the energy of the relative motion of the nuclei (see Ref. 15). In such a case, the differential cross section depends on a specific choice of *two* energies among the set $(E_n, \epsilon, \epsilon')$.
- ²⁵A. F. Starace, in Vol. 31 of *Hanbuch der Physik*, edited by S. Flügge (Springer-Verlag, Berlin, 1982), p. 1.
- ²⁶*Handbook of Mathematical Functions*, edited by M. Abramowitz and I. A. Stegun (Dover, New York, 1965).
- ²⁷D. M. Brink and G. R. Stachler, *Angular Momentum* (Clarendon, Oxford, 1968).
- ²⁸We are indebted to Dr. J.-P. Gauyacq for this remark.
- ²⁹A. Messiah, *Quantum Mechanics* (North-Holland, Amsterdam, 1961).
- ³⁰H. Le Rouzo (unpublished).
- ³¹For bound states, the correlation energy (E_{corr}) is usually defined as the difference $E_{\text{scf}} - E_{\text{exact}}$, where E_{scf} is the (closed-shell) Hartree-Fock energy and E_{exact} the exact (non-relativistic) energy. For He(1^1S_0) one has $E_{\text{scf}} = -2.861\,68$ hartrees [C. J. Roothaan and A. W. Weiss, Rev. Mod. Phys. **32**, 194 (1960)] and $E_{\text{exact}} = -2.903\,72$ hartrees [T. Kinoshita, Phys. Rev. **105**, 1490 (1957)], hence $E_{\text{corr}} = 0.042\,04$ hartrees.
- ³²R. K. Nesbet and R. E. Watson, Phys. Rev. **110**, 1073 (1958). This He(1^1S_0) ground-state wave function gives an energy of $-2.902\,76$ hartrees and accounts for 97.7% of the correlation energy.
- ³³N. Sabelli and J. Hinze, J. Chem. Phys. **50**, 684 (1969).
- ³⁴R. J. Tweed, J. Phys. B **5**, 820 (1972). See also Ref. 13.
- ³⁵J. N. Silverman, O. Platas, and F. A. Matsen, J. Chem. Phys. **32**, 1402 (1960).
- ³⁶R. J. Tweed and J. Langlois, J. Phys. B **20**, 5213 (1987).
- ³⁷The neglect of the *dd* part of the ground-state wave function by BJ can be seen in Eqs. (28) and (29) of Ref. 13, where the coefficients $A^{(2)}$ are missing.
- ³⁸J. M. Bizau, Thèse de troisième cycle, Université de Paris-Sud, 1981; J. M. Bizau, F. Wuillemeunier, D. Ederer, P. Koch, P. Dhez, S. Krummacher and V. Schmidt (unpublished).
- ³⁹T. A. Carlson, Phys. Rev. **156**, 142 (1967).
- ⁴⁰G. Raseev and H. Le Rouzo, *Proceedings of the Thirteenth International Conference on the Physics of Electronic and Atomic Collisions, Berlin, 1983*, edited by J. Eichler, W. Fritsch, I. V. Hertel, N. Stolterfoht, and U. Wille (ICPEAC, Berlin, 1984), p. 36.
- ⁴¹M. Brauner, J. S. Briggs, and H. Klar, J. Phys. B **22**, 2265 (1989).
- ⁴²R. Peterkop, J. Phys. B **15**, L751 (1982).